Published in final edited form as:
J Biomed Mater Res A. 2012 December ; 100(12): 3480–3489. doi:10.1002/jbm.a.34267.

Development of a Mechanically Tuneable 3D Scaffold for Vascular Reconstruction

Maritza Rodriguez[1], **Cassandra Juran**[2], **Mark McClendon**[1], **Cyril Eyadiel**[1], and **Peter McFetridge**[2,*]

[1]School of Chemical Biological and Materials Engineering, University of Oklahoma

[2]J. Crayton Pruitt Family Biomedical Engineering Department, University of Florida

Abstract

Material compliance has been shown to be a predictor of vascular graft patency and as such is a critical parameter when designing new materials. While *ex vivo* derived materials have been clinically successful in a number of applications their mechanical properties are a direct function of the original vessel and are not easily controllable. These investigations describe an approach to modulate the mechanical properties of an *ex vivo* derived scaffold by machining variable (discrete) wall thicknesses to control compliance. Human umbilical arteries (HUA) were machine-lathed directly from the umbilical cord at wall thicknesses of 250, 500, 750, and 1000 μm then decellularized using 1 % sodium dodecyl sulfate (SDS). Compliance over physiological pressures, increased from 3.08±1.84% to 11.47±4.11% as direct function of each discrete vessel diameter. Radial stress strain analysis revealed primary and secondary failure points attributed to the discrete layers within the anisotropic scaffold. Maximum strength and suture retention were shown to increase with increasing wall thickness, by contrast stress failure decreased with increasing thickness due to increasing proportions of the mechanically weaker amorphous Wharton's jelly (WJ). Reseeded smooth muscle cells were shown to adhere, proliferate, and migrate from the scaffold surface showing the potential of the HUA as a mechanically 'tunable' material with applications as an acellular implant or as a tissue engineered construct.

Keywords

artery; *ex vivo* tissue scaffold; smooth muscle cells (SMC); decellularization; compliance

Introduction

The US National Hospital Discharge Survey (NHDS) approximates that 253,000 patients had 448,000 coronary artery bypass surgery procedures in the United States in 2006. While autologous vessels are preferred for peripheral and coronary bypass these may not be available due to disease progression, aged vessels, and anatomical limitations.[1,2] There is also a significant need for smaller diameter grafts for patients that develop plaques in vessels that supply blood to other major organs and periphery of the body.[3] Despite the considerable clinical demand for small diameter blood vessel substitutes there has been limited success with vessels <6mm in diameter, due to a number of potential complications such as early thrombosis, aneurysm formation, anastomotic intimal hyperplasia, and compliance mismatch.[2,4,5,6,7] These clinical outcomes are primarily driven by a high resistance of the vessel walls, as well as low flow rates associated with small diameter replacement vessel.[5]

*Corresponding Author: J. Crayton Pruitt Family Biomedical Engineering Department, University of Florida, JG-56, Biomedical Sciences Building, Gainesville, FL 32611-6131, Phone -(352) 273 9325, Fax -(352) 373 9221, pmcfetridge@bme.ufl.edu.

Aside from synthetic materials, research is actively being conducted on xenogeneic and allogeneic alternatives due to their inherent biological advantages. Biologically derived materials not only have structural advantages, but contain important biological molecules such as: glycosaminoglycans, proteins, growth factors, and proteoglycans, all which can facilitate cellular adhesion and extracellular matrix remodelling to aid tissue regeneration. There has been promising research using allografts and xenografts using materials such as human umbilical vein grafts, porcine carotid arteries, porcine small intestinal submucosa (SIS).[8,910,11,12,13,]

Vascular scaffolds derived from human umbilical arteries and veins have a number of interesting properties that may be exploited. Of particular interest to these works are the structure and composition of the adventitia/connective tissues that surround the vessel proper, the 'Wharton's Jelly' (WJ). This component of the scaffold is rich in glycosaminoglycans (GAGs), peptide growth factors (PGF), and proteoglycans, which may provide a rich environment conducent for scaffold remodelling.[14, 15,16] Similar in structure and with the same derivation as the HUA, the human umbilical vein (HUV) has had positive clinical results over the past three to four decades as a glutaraldehyde cross-linked implant.[12,13] While being resistant to degradation, natural materials cross-linked in this manner lack the capacity to remodel into functional vessels. Also using the HUV, Daniel and McFetridge *et al* developed a novel dissection method to automate dissection of the vein from the umbilical cord using a modified lathe that results in a vessel with a more uniform surface at a specified thickness.[17] This approach reduces lengthy manual dissection times and improves uniformity of the dissected vessel with a reproducible wall thickness. The automated dissection technology has been extended to the HUA.

Although similar to the human umbilical vein, the human umbilical artery provides an alternative material as a replacement for smaller blood vessels due to having a smaller diameter and a more robust medial layer structure.[18] This study investigates the potential of the human umbilical artery as a mechanically tuneable substitute blood vessel. Mechanical tests performed on lathed, decellularized vessels compared with the manually dissected tissue (control) gave insight on how the vessel can be customized to have specific mechanical properties by controlling wall thickness (250μm to 1000μm). With mechanical matching of graft materials to the natural vasculature a high priority, the ability to custom-tune scaffold mechanics to avoid compliance mismatching may improve patency rates in comparison to other high modulus materials.

Materials & Methods

Automated dissection

Deidentified human umbilical cords (Fig. 1A, B) were obtained from Norman Regional Hospital. Vessels were cleaned and used within 24 hours of collection. Once machined and processed (decellularization and sterilization) vessels were seeded or used for mechanical testing within 24 hours. During intermittence vessels were stored at 4°C in phosphate buffer saline (PBS, pH 7.4). Each 10 cm section of the whole umbilical cord was mounted on a stainless steel mandrel (3.5 mm OD) inserted through the artery lumen (Fig. 1C). Mounted tissues were then progressively frozen at a rate of 2.5°C/min to −86 °C in a styrofoam container. After a minimum of twelve hours, the mounted, frozen vessels (Fig. 1D) were removed and immediately inserted into a custom-built Micro-kinetics computer numerical control (CNC) lathe (Kennesaw, GA) (Fig. 2A). Tissues were cut at a rotational speed of 2900rpm (Fig. 2B, C) at thicknesses of 250, 500, 750, or 1000 μm(Fig. 3) yielding arteries with a smooth surface and a uniform thickness (Figs. 1E, 2D). Dissected arteries were then thawed in double-distilled water at 5°C for 1 hour before decellularization.

Manual Dissection

A steel rod (3.5 mm OD) was inserted through the artery lumen, then the tissue surrounding the artery was dissected away using a scalpel. This resulted in vessels with wall thicknesses ranging between 200 and 350 μm.

Decellularization

After dissection and thawing, arteries were immersed in 1% (w/v) sodium dodecyl sulfate (SDS) for 24 hours on an orbital shaker (100rpm), rinsed in distilled water for 24 hours, washed for 24 hours in 75% ethanol, then washed again in distilled water. Samples were sterilized using 0.2% peracetic acid for 2 hours, rinsed in distilled water, then rinsed in PBS for 24 hours until pH balanced at 7.2. Decellularized arteries were stored in sterile PBS at 5°C prior to use. Manually dissected HUAs were not decellularized to maintain the natural properties of the tissue.

Stress-Strain Testing

Artery ringlets (5mm wide) were loaded onto a uniaxial tensile testing rig (Instron Corp, Instron 5543 testing machine, Norwood, MA) using stainless steel L-shaped hooks. To determine the stress-strain relationship and yield stress in the radial direction, an initial force of 0.005N was applied to the sample ringlet, after which the rings were extended until failure at a rate of 5mm/min. The strain was calculated from the initial diameter of the ringlet (L_I) and the extension induced by the mechanical testing machine (change in the ringlet diameter ($L_F - L_I$) where L_F is the extension at failure) using the equation $\varepsilon = \frac{(L_F - L_I)}{L_I}$. The resulting tensile stress was calculated using $\sigma = \frac{F}{(2tw)}$, where $2tw$ the cross sectional area of the ringlet the force was applied with t being the ringlets thickness and w the width of the ringlet in contact with the hooks.

For the longitudinal stress strain analysis, arteries were cut into flat sheets (10mm wide x 30mm long) and clasped on each end by mechanical grips. Strain was computed as above except L_I represents the initial longitudinal length and L_F was the longitudinal length of the strip at failure. Stress was then determined using $\sigma = \frac{F}{tw}$, with t the strip thickness and w the strip width equal to 10mm.

Suture Retention

Suture holding capacity was assessed by applying uniaxial force (Instron Corp, Instron 5543 testing machine, Norwood, MA) to sutured samples cut longitudinally to form a 10 mm wide × 30 mm long sheet. A single sterile 3–0 braided silk suture was passed through one end of the tissue section 3 mm below the cut edge, with the other attached to the test rig. Samples were preloaded to a force of 0.005 N and then an extension rate of 5 mm/min was applied until failure.

Burst Pressure and Compliance Analysis

2.5cm sections of HUA were used to test vessels compliance and burst failure using a Master Test Type 220-4s pressure transducer (Mash Instrument Company, Skokie, IL) and a syringe pump with an in-flow rate of 60ml/min. For compliance, the diameter of each artery was measured using image analysis software (ImageJ, Image Processing and Analysis in Java) of video stills recorded during testing at 80 and 120 mmHg. Compliance was calculated by multiplying the percent diameter change with the inverse difference in pressure.[17]

$$compliance = \frac{\Delta D}{D_0 \Delta P} = \frac{(D_{P2} - D_{P1})}{D_{P1}(P_2 - P_1)}$$

SEM

Samples of lumenal and ablumenal artery surfaces were gently washed three times in PBS, fixed in 1%(v/v) glutaraldehyde for 4 hours, rewashed three times in PBS, soaked in 1% osmium in PBS for 2 hours, washed, and dehydrated in graded ethanol treatments (30%, 50%, 70%, 90%, 95%, and 100%) for 10 minutes each. Samples were then critical point dried, gold sputtered, and analyzed using a JEOL LSM-880 Scanning Electron Microscope at 15 kV.

Cell culture

Human smooth muscle cells (#2854) were purchased from ATCC (Manassas, VA) and cultured under standard conditions at 37°C with a 5% CO_2 concentration. Media was composed of Dulbecco's Modified Eagle's Medium (DMEM) containing 10% fetal serum complex (Gemini Bio-Products, West Sacramento, CA) and 1% penicillin/streptomycin (Gibco Life Technologies, Grand Island, NY). After artery decellularization, arteries were cut longitudinally, opened and cut into circular disks using a 5/16″ steel punch (scaffold surface area = 49.5 mm^2). Scaffolds were then soaked in media and incubated at 37°C, 5% CO_2 overnight prior to seeding. Smooth muscle cells, suspended in media, were seeded in onto the ablumenal surface of the scaffold at a density of 1200 cells/mm^2 and cultured to assess initial scaffold interactions over 10 days.

Cell Metabolism and Concentration

Three control scaffolds and three seeded scaffolds were sampled at 2 hours, 1 day, 5 days and 10 days of culture to assess cellular metabolism and DNA content. Cellular metabolism was characterized using the REDOX compound resazurin (Alamar Blue assay, Biosource International, Camarillo, CA). Briefly, scaffolds were rinsed gently in PBS, transferred into new wells, and Alamar blue dye and media were added into the well in a 1:10 concentration ratio for 6 hours. Absorbance was measured at wavelengths of 570nm and 600nm in order to calculate Alamar Blue reduction, which is a measure of reduction reactants of cellular metabolism. Samples were then frozen, cut into small sections, and degraded by overnight incubation in collagenase (Sigma-Aldrich Inc., St. Louis, MO) in PBS at 37°C. Afterwards, samples were sonicated to ensure all DNA was released from the cells. Once samples were homogenous, a Pico Green florescence assay (Invitrogen, Carlsbad, CA) was performed to determine scaffold DNA concentration, as per manufactures instructions. DNA content is proportional to cell concentration and the combination of Pico Green and Alamar Blue assays allows for determination of the average metabolism per cell at each time point.

Histology

Scaffolds were fixed in 10% buffered formalin overnight, processed, and embedded in paraffin. Samples were cut to 5 μm, mounted and stained with H&E as per standard protocols. The stained tissue cross-sections were analyzed using a light microscope (Nikon, Eclipse E800).

Statistical Analysis

All statistics were performed using SPSS software. All comparisons were made using one way ANOVA and the post hoc Tukey test establishing significance with p value 0.05 or less for sample size greater than or equal to three as indicated.

Results

Automated Dissection & Decellularization Method Evaluation

The automated dissection of the HUA from the umbilical cord using the CNC lathe resulted in a vessel with a smooth surface and uniform wall thickness (Figs. 1E and 2D). Manually dissected arteries (controls) had visibly rough, uneven surfaces and thicknesses varying from approximately 250–350 μm (Fig. 3). Figure 4 shows an SEM of the scaffolds cross-section, displaying typical arterial structure with the addition of the Wharton's jelly surrounding the vessel adventitia. Histology images in Figure 5 show the structure of a native HUA to be consistent with other blood vessels having a lumenal surface composed of tightly packed extracellular matrix proteins and more loosely packed ECM fibers on the ablumenal side. Figures 5A and 5D, respectively, reveal the surface morphology of the lumen of native tissue as compared to decellularized artery scaffolds, which have maintained the tightly packed ECM structure. The ablumenal surface shown in Figures 5B and 5C, had more loosely packed fibers grouped in a structured manner, whereas after decellularization (Fig. 5E, F), these fibers became more loosely packed and with a decrease in structural organization.

Mechanical Properties of the Human Umbilical Artery Scaffold

Tensile Testing—Typically radial tensile testing on 5mm wide ringlets of various thicknesses yielded two distinctive failure points (Fig. 6). The primary failure points for decellularized arteries occurred at similar extension lengths, between 3.2 – 4.4 mm, for all scaffold thicknesses. The primary failure peak was over a force range of 5.93 – 7.72 N, most of which were not significantly different from that of the manually dissected arteries (5.62 ± 0.81 N). This failure point is attributed to the vascular media layer, which remained constant for all thicknesses, and unaffected by the lathing process. Relative to the primary failure point, a secondary failure point was observed that occurred over a wider displacement range, between 5.4 – 9.9 mm. Failure peaks displayed a statistically significant increase in stress from 1.14 to 6.05 N as the vessels overall thickness increased (Fig. 7).

Longitudinal force displacement tests on the flat artery sheets revealed only one tensile strength failure point per sample ranging from 1.50 – 22.01 N. The strength increased with increasing scaffold wall thickness reaching a maximum force value at 750 μm (Fig. 8), with no significant difference between the 750 μm and 1000 μm thick scaffolds. The variation in strength with increasing thickness implies the WJ layer is the main component responsible for the mechanical properties in the longitudinal direction. The manually dissected tissue, with layers exterior to the media removed, displayed a similar tensile strength as the 250 μm thick decellularized scaffolds. However, there was an increase in strength observed for the thicker decellularized scaffolds.

Suture Retention—As shown in Figure 9, thicker tissues displayed significantly higher values for suture retention. The suture holding capacity for all samples ranged from 0.56 – 1.83 N, with no difference in suture holding capacity between 750μm and 1000μm thick scaffolds.

Stress Description—The stress values for radial and longitudinal analyses are reported in Figure 10. Manually dissected tissue and the decellularized tissue at a 250μm wall thickness had similar stress values as they had similar thicknesses. Contrary to the direct force displacement measurements, the radial stress decreases with increasing thickness at the primary failure points and remains approximately equal for the secondary failure points across all thicknesses.

Burst Pressure & Compliance—In order to examine the capability of this scaffold to withstand high blood pressure in the body, the burst pressures of scaffolds with varying thicknesses were assessed. Burst pressures ranged from 585–1570 mmHg, with thinner artery scaffolds resulting in lower burst pressures than those over 500 μm (Fig. 11). The compliance of the scaffold over the 80/120 mmHg pressure range decreased with increasing thickness (Table 1). Compliance values of other materials being studied as small diameter blood vessels are shown in Table 2.

Initial cellular interactions and scaffold remodeling—Prior to seeding, the decellularized scaffolds displayed no sign of cell nuclei throughout the vessel, see Figure 12A. Removal of whole cells by the decellularization process was confirmed with non-seeded controls (Fig. 12A). Seeded cells attached and proliferated on the ablumenal surface as indicated by the hematoxylin and eosin stained cross-sections (Fig. 12B), but markedly proliferation was most visible after 10 days, where cells had migrated up to 100 um into the scaffold (Fig. 12C). Approximately 60,000 cells were seeded onto each disk and results showed 4,300 cells present one day after seeding (Fig. 13). There was an average of 66,000 cells after 5 days and 294,000 cells after 10 days of culture. Results showed that after 10 days of culture, cells attach and proliferate on the ablumenal surface of the scaffold, with Alamar Blue reduction showing an increase in the bulk cellular metabolism (Fig. 13). Shown on the secondary y-axis is the percent metabolism per cell which was calculated using cell density data to give the metabolic activity per-cell. These data show cell activity to increase significantly after one day to day 5, and then decrease until day 10.

Discussion

In these investigations we provide a characterization of the structural, biomechanical, and *in vitro* biocompatibility of prepared HUA with tunable vessel compliance in order to assess its potential as an acellular graft or tissue engineered construct.

In contrast to time-consuming, error-prone manual approaches to dissect the blood vessels from the human umbilical cord,[19,20,21] the automated dissection method allows a specific wall thickness[22] to be “dialed-in” yielding an artery with a relatively smooth and uniform surface within 1–2 minutes.[17] Key to this approach is the ability to dissect the HUA with specific wall thicknesses such that the vessels mechanical characteristics can be tuned to a specific range of properties. This is of particular importance in matching vessel compliance where failure to do so has been linked to vessel failure.[23] A major hemodynamic consequence of compliance mismatch is low shear stress rates, turbulence, disturbed flow, decreased distal perfusion and increased impedance which leads to the occurrence of intimal hyperplasia that can result in graft occlusion.[24] In addition to variable cellular responses to changes in compliance (differential wall strain values), reduced compliance also results in a local increase in blood pressure and velocity due to reduced vessel expansion.[25] Using the data from various studies, it has been shown that as the compliance discrepancy increases, patency decreases. As reported by Zilla *et al*, native arterial compliance was 0.059 ± 0.005 %/mmHg, with the umbilical vein graft having the highest patency of 75% (compliance = 0.037 ± 0.005 %/mmHg), Dacron patency was 50% (compliance = 0.019 ± 0.003%/mmHg), and PTFE had a further reduced patency rate of 40% (compliance = 0.016 ± 0.002 %/mmHg).[26,27,28]

Since the HUA’s extracellular matrix allows for the preparation of scaffolds at different thicknesses, and results show a decrease in compliance with increasing thickness, a vessel can be “tuned” to match the compliance needed on a patient-to-patient basis (or vessel specific basis). The ability to provide a material that can be manipulated to provide a range

of compliance values is important since the vessel compliance decreases with increasing age, and even more so when medial calcification and arteriosclerosis occur.[29]

Scaffolds dissected to 500 and 750μm wall thicknesses had similar compliance values to porcine carotid arteries (0.187± 0.041 %/mmHg)[30] and thicker scaffold values were similar to the human saphenous vein (0.04 %/mmHg)[31] and femoral artery (0.06 %/mmHg).[31] Although compliance values were generally high, the percent diameter change,[32] was within the general 1–10% range of biological materials used for small diameter vascular grafts,[17,33,34] with the exception of the carotid, femoral and iliac values (15%) measured by Dobrin *et al.*[35] The percent diameter change reported for synthetic materials PTFE and Dacron were below 1%.[36]

In order to be successful vascular grafts are required to withstand physiological blood pressures for extended periods. Burst pressure (P_B) increased significantly (Fig. 11) with scaffold wall thicknesses of 500μm and above. Gui *et al.* found slightly higher burst pressures for manually dissected non-decellularized HUA's (969.66 ± 154.42 mmHg) compared to decellularized HUA's (840.37±114.67 mmHg), but there was no significant difference between the two.[18] Our study's decellularized vessels had higher P_B's (605.66 ± 262.99 mmHg) than non-decellularized manually dissected vessels (585.79 ± 151.29 mmHg) but were also not significantly different. However, for this particular thickness (250μm) the P_B values in this study are 300 mmHg lower than those found in Gui's study. This may be due to inherent inconsistencies of the manual dissection approach where thicknesses can be over (or under) stated. Overall, the burst pressures for thinner HUA scaffolds (250 μm) were similar to reported values of synthetic scaffolds (Table 2), whereas those for thicker HUA scaffolds (>500 μm) were significantly higher, but lower than several native arteries and veins.

While the outer layers of the HUA clearly contribute to the vessels' P_B, the primary mechanical strength is provided by the medial layer, (approximately 250–350μm thick). Therefore, with larger diameters, the contribution of the medial layer was reduced relative to the Wharton's jelly zone. All P_B's remained significantly higher than physiological and hypertension values, showing these vessels have suitable structural integrity at physiological pressures. For comparison purposes the burst pressures of various materials being studied for use as a small diameter vascular graft have noted, see Table 2.

The HUA is a composite material and as such behaves in an anisotropic fashion. We hypothesized that the primary failure point was due to the failure of the medial layer, as it was unchanged across all scaffold thicknesses, and with adventitia and connective tissue composed of the less structurally defined Wharton's Jelly accounting for the secondary failure point. Figure 10 illustrates that thinner scaffolds have higher primary failure stress values as they are composed of a higher ratio of the medial layer per unit area relative to the thicker scaffolds containing a lower ratio of strong medial layer to the larger cross sectional area due to inclusion of WJ, that was shown to be a mechanically weaker material.

An analysis of the early *in vitro* cell interactions with the modified arterial scaffold was designed to assess early cellular interactions. Histology shows the SDS decellularization method left no visible cells, with reseeded SMCs visible on recellularized scaffolds after ten days of culture. Cells were visible initially as a monolayer that over time migrated approximately up to 100μm into the scaffold forming a multi-layer around the scaffolds peripheral surface. Metabolic activity showed an initial spike in activity (on a per cell basis) then decreased after 5 days and remained constant after 10 days of culture. This is possibly due to an initial period where cells acclimate to the new conditions then go into a period of reduced activity (Fig. 13). While these investigations were limited in time scale to show

early remodeling events it was clear that SMC populated the ablumenal surface and increased in cell density. These results indicate that the base scaffold has sufficient biological and material properties to support cellular proliferation and scaffold remodeling.

In summary, we have developed a rapid automated dissection method with the ability to customize vessel wall thickness in order to modulate compliance. The scaffold has shown its potential to support the adhesion and proliferation of cells as well as ECM remodeling. Future studies will incorporate a three dimensional bioreactor to mimic the host environment on the HUA seeded with endothelial cells on the lumenal surface and smooth muscle cells on the ablumenal surface. These investigations in concert with future *in vivo* analysis will provide additional validation of the importance of compliance, and insight to biological tissue remodeling. The HUA is a promising material as a small diameter cardiovascular graft, with the capacity to modulate mechanical properties to suit the demands of differing vascular locations.

Acknowledgments

Funding in part is by National Institute of Health R01 HL088207, and the Graduate Assistance in Areas of National Need Fellowship from the U.S. Department of Education, with matching funding from the University of Oklahoma.

References

1. Konig G, McAllister TN, Dusserre N, Garrido SA, Lyican C, Marini A, Fiorillo A, Avila H, Wystrychowski W, Zagalski K, Maruszewski M, Jones AL, Cierpka L, de la Fuente LM, L'Heureux N. Mechanical properties of completely autologous human tissue engineered blood vessels compared to human saphenous vein and mammary artery. Biomaterials. 2009; 30:1542–1550. [PubMed: 19111338]
2. Zhang W, Liu W, Cui L, Cao Y. Tissue engineering of blood vessel. J Cell Mol Med. 2007; 11(5): 945–957. [PubMed: 17979876]
3. American Heart Association Heart Disease and Stroke Statistics – 2009. p Available at: http://circ.ahajournals.org/cgi/reprint/CIRCULATIONAHA.108.191261
4. Isenberg BC, Williams C, Tranquillo RT. Small-Diameter Artificial Arteries Engineered In Vitro. Circ Res. 2006; 98:25–35. [PubMed: 16397155]
5. Brewster, L.; Brey, EM.; Greisler, HP. Principles of Tissue Engineering. 3. Elsevier Inc; 2007.
6. Hoenicka M, Lehle K, Jacobs VR, Schmid FX, Birnbaum DE. Properties of the Human Umbilical Vein as a Living Scaffold for a Tissue-Engineered Vessel Graft. Tissue Engineering. 2007; 13(1): 219–229. [PubMed: 17518595]
7. Ballyk PD, Walsh C, Butany J, Matadial O. Complicance mismatch may promote graft-artery intimal hyperplasia by altering suture-line stresses. Journal of Biomechanics. 1998; 31:229–237. [PubMed: 9645537]
8. McFetridge PS, Daniel JW, Bodamyali T, Horrocks M, Chaudhuri JB. Preparation of porcine carotid arteries for vascular tissue engineering applications. J Biomed Mater Res. 2004; 70A:224–234.
9. Schmidt CE, Baier JM. Acellular vascular tissues: natural biomaterials for tissue repair and tissue engineering. Biomaterials. 2000; 21:2215–2231. [PubMed: 11026628]
10. Dardik H. The second decade of experience with the umbilical vein graft for lower-limb revascularization. Cardiovascular Surgery. 1995; 3(3):265–269. [PubMed: 7655839]
11. Dardik H, Miller N, Dardik A, Ibrahim IM, Sussman B, Barry SM, Wolodiger F, Kahn M, Dardik I. A decade of experience with the glutaraldehyde-tanned human umbilical cord vein graft for revascularization of the lower limb. J Vasc Surg. 1988; 7:336–346. [PubMed: 3123718]
12. Dardik I, Dardik H. Vascular Heterograft: Human Umbilical Cord Vein as an Aortic Substitute in Baboon. J Med Prim. 1973; 2:296–301.
13. Dardik H, Ibrahim IM, Sprayregen S, Dardik II. Clinical experience with modified human umbilical cord vein for arterial bypass. Surgery. 1976; 76(6):618–624. [PubMed: 1273747]

14. Gogiel T, Bankowski E, Jaworski S. Proteoglycans of Wharton's jelly. The International Journal of Biochemistry & Cell Biology. 2003; 35:1461–1469.
15. Sobolewski K, Bankowski E, Chyczewski L, Jaworski S. Collagen and glycosaminoglycans of Wharton's Jelly. Biology of the Neonate. 1997; 71:11–21. [PubMed: 8996653]
16. Sobolewski K, Malkowski A, Bankowski E, Jaworski S. Wharton's jelly as a reservoir of peptide growth factors. Placenta. 2005; 26:747–752. [PubMed: 16226124]
17. Daniel J, Koki A, McFetridge PS. Development of the Human Umbilical Vein Scaffold for Cardiovascular Tissue Engineering Applications. ASAIO Journal. 2005; 51(3):252–261. [PubMed: 15968956]
18. Gui L, Muto A, Chan SA, Breuer CK, Niklason LE. Development of Decellularized Human Umbilical Arteries as Small-Diameter Vascular Grafts. Tissue Engineering: Part A. 2009; 15(9): 2665–2676. [PubMed: 19207043]
19. Yeh W-S, Keller JT, Brackett KA, Frank E, Tew JM. Human umbilical artery for microvascular grafting: Experimental study in the rat. J Neurosurg. 1984; 61:737–742. [PubMed: 6470785]
20. Vlessis AA, Hovaguimian H, Arntson E, Starr A. Use of Autologous umbilical artery and vein for vascular reconstruction in the newborn. The Journal of Thoracic and Cardiovascular Surgery. 1995; 109:854–857. [PubMed: 7739244]
21. Kerdjoudj H, Boura C, Marchal L, Dumas D, Schaff P, Voegel J-C, Stoltz J-F, Menu P. Decellularized umbilical artery treated with thin polyelectrolyte multilayer films: Potential use in vascular engineering. Bio-Medical Materials and Engineering. 2006; 16:S123–S129. [PubMed: 16823103]
22. Crouzier T, McClendon T, Tosun Z, McFetridge PS. Inverted human umbilical arteries and tunable wall thicknesses for nerve regeneration. J Biomed Mater Res A. 2009; 89(3):818–828. [PubMed: 18615471]
23. Seifalian, AM.; Giudiceandrea, A.; Schmitz-Rixen, T.; Hamilton, G. Non-compliance: The silent acceptance of a villain. In: Zilla PaG, PH., editor. Tissue Engineering of Prosthetic Vascular Grafts. R G Landes Company Publishers; 1998. p. 43 -56.
24. Baird RN, Abbott WM. Pulsatile blood flow in arterial grafts. The Lancet. 1976; 30:948–949.
25. Kerdjoudj H, Boura C, Moby V, Montagne K, Schaaf P, Voegel J-C, Stoltz J-F, Menu P. Re-endothelialization of Human Umbilical Arteries Treated with Polyelectrolyte Multilayers: A Tool for Damaged Vessel Replacement. Adv Funct Mater. 2007; 17:2667–2673.
26. Veith FJ, Gupta SK, Ascer E, White-Flores S, Samson RH, Scher LA, Towne JB, Bernhard VM, Bonier P, Flinn WR, Astelford P, Yao JST, Bergan JJ. Six year prospective multicenter randomized comparison of autologous saphenous vein and expanded polytetrafluoroethylene grafts in infrainguinal arterial reconstructions. J Vasc Surg. 1986; 3:104–114. [PubMed: 3510323]
27. Taylor LM, Edwards JM, Porter JM. Present status of reversed vein bypass grafting: five years result of a modern series. J Vasc Surg. 1990; 11(2):193–205. [PubMed: 2299743]
28. Dardik H, Ibrahim IM, Dardik I. Evaluation of glutaraldyhyde tanned human umbilical cord vein as a vascular prosthesis for bypass to the popliteal, tibial and peroneal arteries. Surgery. 1978; 83(5):577–588. [PubMed: 417413]
29. Schmitz-Rixen, T.; Hamilton, G. Compliance: A critical parameter for maintenance of arterial reconstruction?. In: Greenhalgh, RMHL., editor. The maintenance of arterial reconstruction. London: WB Saunders; 1991. p. 23-43.
30. Dahl SLM, Rhim C, Song YC, Niklason LE. Mechanical Properties and Compositions of Tissue Engineering and Native Arteries. Annals of Biomedical Engineering. 2007; 35(3):348–355. [PubMed: 17206488]
31. Hastings, GW. Cardiovascular biomaterials. London: Springer; 1992.
32. Conklin BS, Richter ER, Kreutziger KL, Zhong D-S, Chen C. Development and evaluation of a novel decellularized vascular xenograft. Medical Engineering & Physics. 2002; 24:173–183. [PubMed: 12062176]
33. Roeder R, Wolfe J, Lianakis N, Hinson T, Geddes LA, Obermiller J. Compliance, elastic modulus, and burst pressure of small-intestine submucosa (SIS), small-diameter vascular grafts. J Biomed Mater Res. 1999; 47:65–70. [PubMed: 10400882]
34. Sawyer, P. Modern vascular grafts. New York: McGraw-Hill Inc; 1987.

35. Dobrin PB. Mechanical properties of arteries. Physio Rev. 1978; 58(2):397–460.
36. Stewart, SFC.; Lyman, DJ. Essential physical characteristics of vascular grafts. In: Sawyer, PN., editor. Modern vascular grafts. New York: McGraw-Hill, Inc; 1987. p. 117-121.
37. Huynh T, Abraham G, Murray J, Brockbank K, Hagen PO, Sullivan S. Remodeling of an acellular collagen graft into a physiologically responsive new vessel. Nat Biotechnol. 1999; 17(11):1083–1086. [PubMed: 10545913]
38. Niklason LE, Gao J, Abbott WM, Hirschi KK, Houser S, Marini R, Langer R. Functional arteries grown in vitro. Science. 1999; 284:489–493. [PubMed: 10205057]
39. L'Heureux N, Paquet S, Labbe R, Germain L, Auger FA. A completely biological tissue-engineered human blood vessel. The FASEB Journal. 1998; 12:47–56.
40. Kambric, HE.; Kantrowitz, A.; Sung, P. American Society for Testing and Materials. Vol. 04-898000-54. Philadelphia: 1984. Vascular graft update.
41. Liu, G-f; Yang, D-p; Han, X-f; Guo, T-f; Hao, C-g; Ma, H.; Nie, C-l. Decellularizaed aorta of fetal pigs as a potential scaffold for small diameter tissue engineered vascular graft. Chin Med J. 2008; 121(15):1398–1406. [PubMed: 18959117]

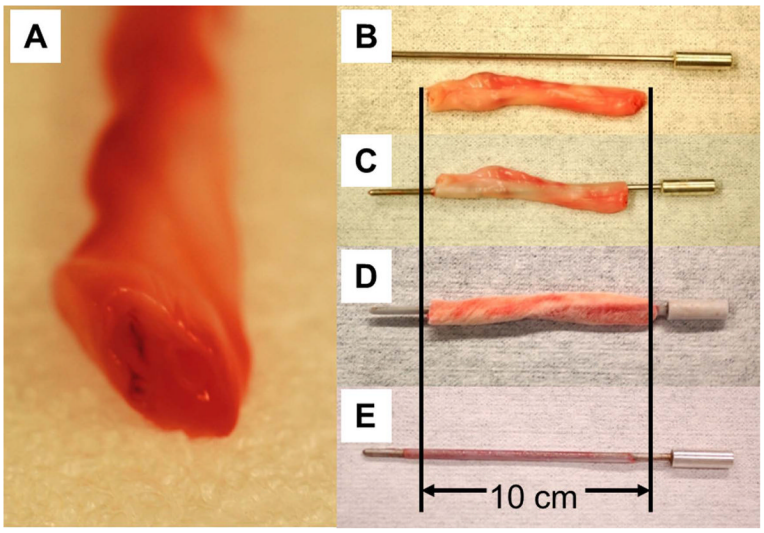

Figure 1. Autodissection of the HUA

(A,B) A section of the human umbilical cord (C) with a stainless steel mandrel inserted into an artery. (D) The cord is frozen at −80°C for a minimum of 12 hours preceding (E) autodissection of the artery.

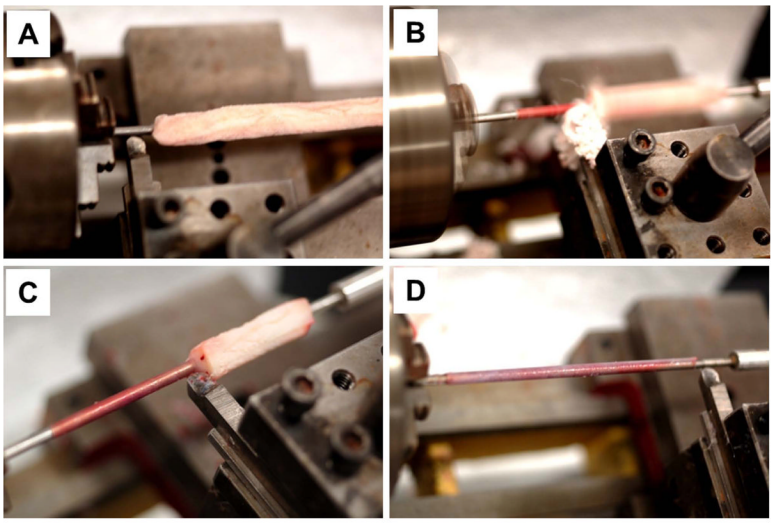

Figure 2. Autodissection Process

The entire umbilical cord is mounted on a stainless steel mandrel and frozen at −80°C. (A) The cord/mandrel construct is then placed on the modified lathe (B and C) and dissected using a high speed cutting tool (D) to produce a dissected artery with a smooth, uniform surface.

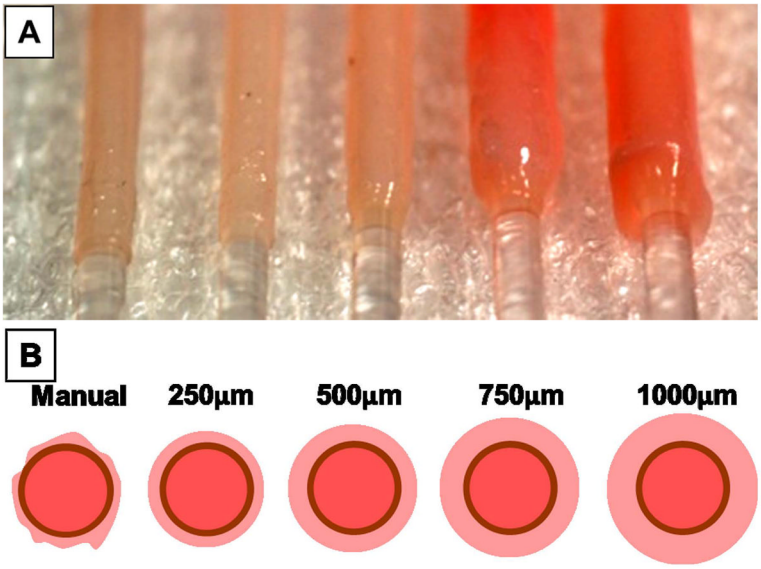

Figure 3. Dissected HUAs of varying thickness

(A) Autodissected and manually dissected HUAs of varying thickness. (B) Cross sectional schematic of the HUAs corresponding to the photo above. Manually dissected tissue had no specific thickness. Autodissected tissue had thicknesses of 200mm, 500mm, 750mm, and 1,000mm.

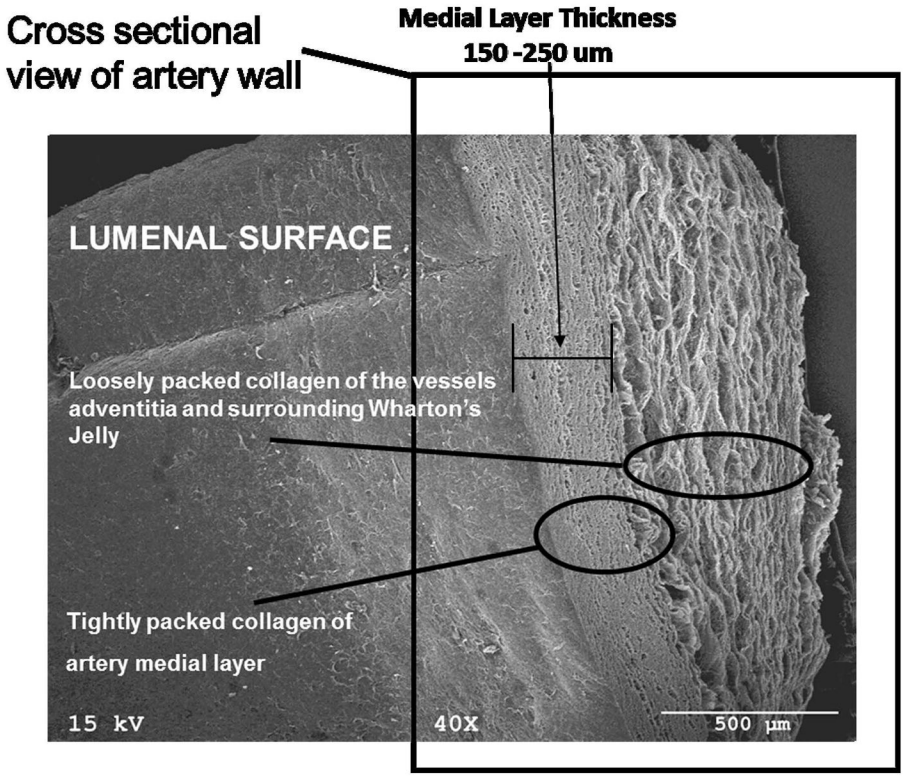

Figure 4. SEM of the HUA

The scanning electron micrograph of the artery wall at a magnification of 40x. The left side of the image shows the tightly packed lumen, whereas the right side shows the loosely packed ablumen.

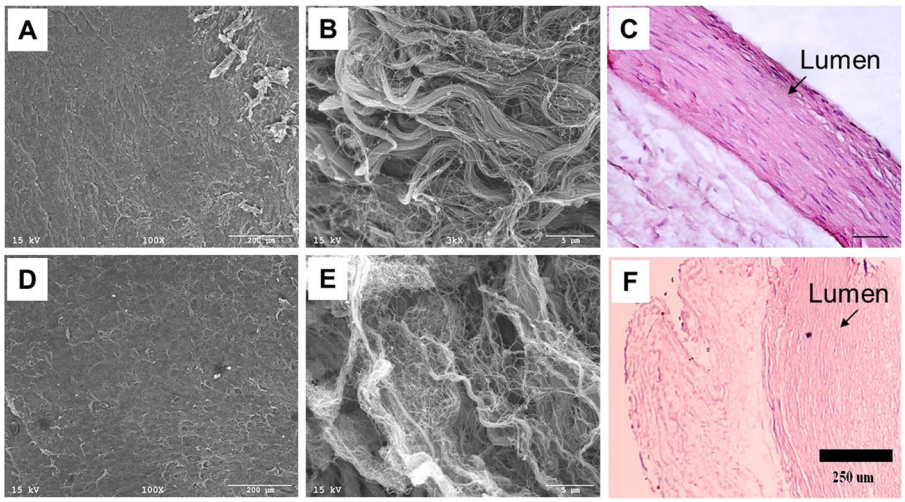

Figure 5. SEM & H&E of the HUA

(A,B,C) The scanning electron micrograph and hematoxylin and eosin staining of the human umbilical artery before decellularization show a more orderly structure of fibers. (D,E,F) The decellularized human umbilical arterial fibers have been unwoven and now show a more loosely-packed, slightly randomized structure.

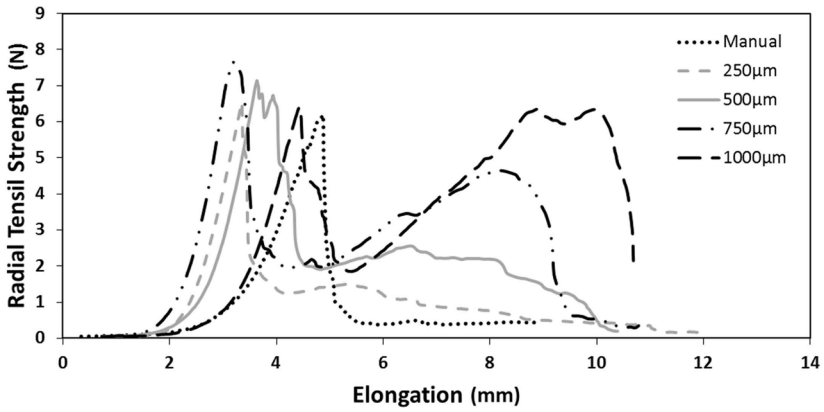

Figure 6. Representative Force Displacement Analysis

Decellularized scaffolds cut into 5mm wide ringlets at various thicknesses were extended at an extension rate of 5mm/min using a force of 0.005N. Primary failure points are attributed to the media layer, which is equivalent for all thicknesses, and the secondary failure is due to the varying thicknesses of the adventitia (Wharton's Jelly).

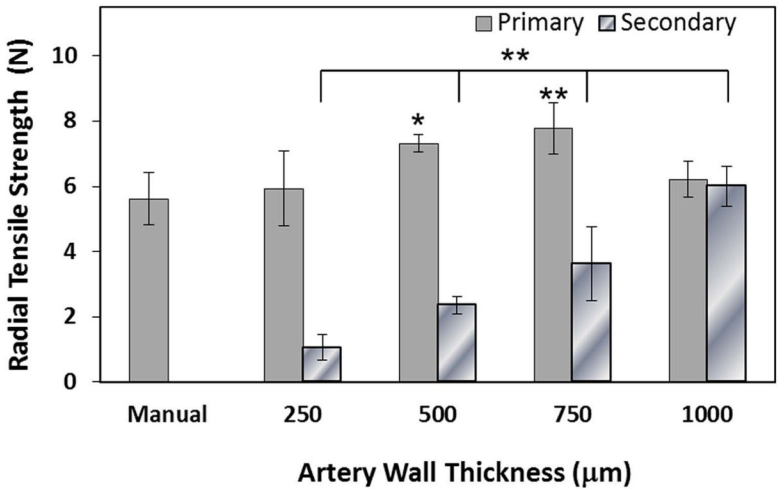

Figure 7. Radial Tensile Strength

The force (g) exerted by the 5mm wide ringlets at the primary and secondary failure points of the manually dissected and autodissected tissue with respect to artery wall thickness (mm). Primary failure points showed difference only between manually dissected and decellularized 500 μm thickness and 750 μm thickness. There was no difference between decellularized scaffolds, whereas all secondary points were significantly different. *p<0.05, **p<.01 (n=4, ANOVA)

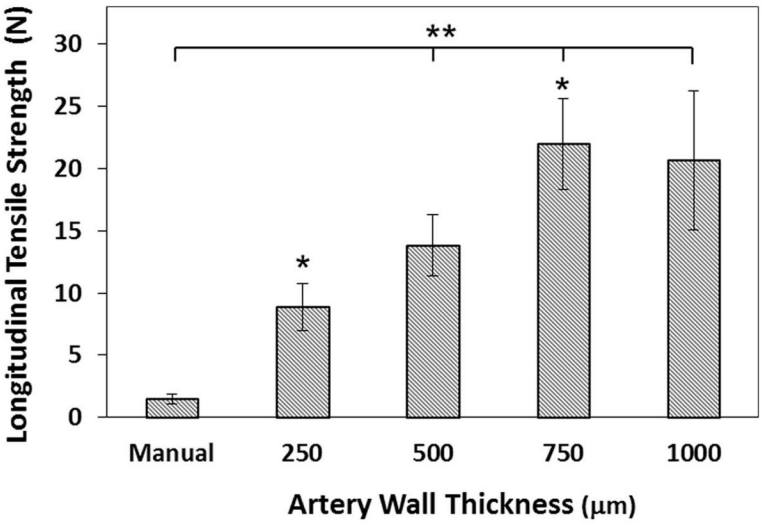

Figure 8. Longitudinal Tensile Strength

HUA scaffolds of varying thicknesses (manual, 250um, 500um, 750um, 1,000um) were cut into flat sheets (10×30mm) and extended until failure. The manually dissected samples show significant longitudinal tensile strength difference from all the decellularized samples except the 250μm thickness. Difference between the decellularized samples only occur between 250 and 750 μm thicknesses *p<0.05, **p<.01 (n=4, ANOVA).

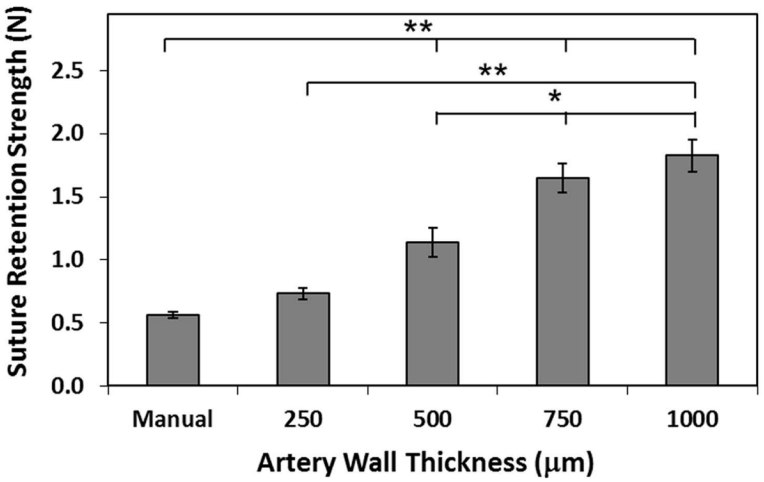

Figure 9. Suture Retention Strength

The suture retention strength (N) of manually dissected and autodissected tissue increased with increasing artery scaffold thickness. Manual dissection showed significant difference between all decellularized thicknesses but 250μm thickness. *p<0.05, **p<0.01 (n=4, ANOVA)

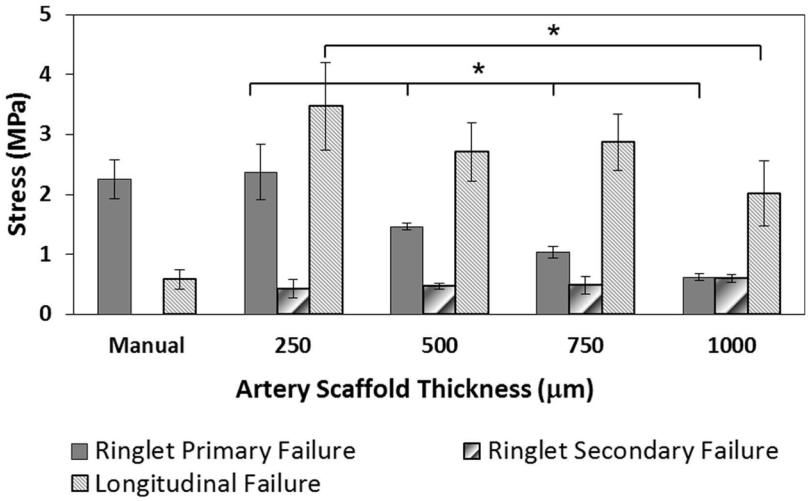

Figure 10. Stress Measurement

A comparison of stress values for each scaffold thickness using the various mechanical testing methods: radial, longitudinal, and tensile testing. Due to the anisotropic property of the material, stress values were examined using cross-sectional areas. *$p<0.05$ ($n\geq3$, ANOVA)

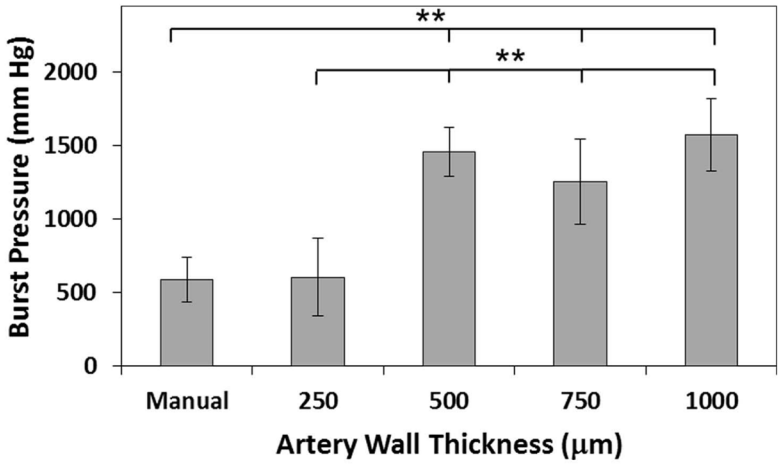

Figure 11. Burst Pressure

The burst pressure (mmHg) results for manually dissected and autodissected arteries showed a dramatic increase at 500um. **p<0.01 (n=12, ANOVA)

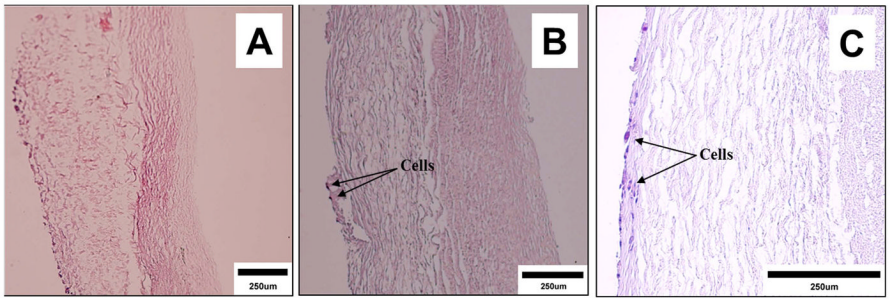

Figure 12. HUA cell seeding, proliferation, and migration

Cross-sectional view of the HUA disk showing the ablumen on the left and the lumen on the right.(A) Day1 decellularized, control tissue shows no cells within the ECM. (B) Day 1 recellularized, difficult to see cellular attachment. HUA scaffolds seeded with cells and cultured for 10 days (C) show a layer of adhered cells on the ablumenal surface migrating approximately 100μm into the scaffold.

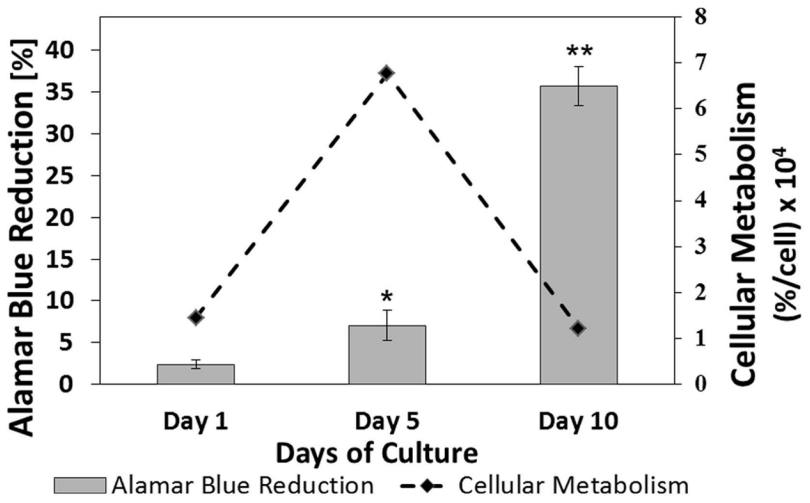

Figure 13. Alamar Blue Reduction & Cellular Metabolism

Reduction of the alamar blue dye was calculated by measuring the absorbance at wavelengths of 570nm and 600nm after 6 hours of incubation of the seeded and control disks with the dye. The 2 hour time point showed minimum cellular metabolism, and there was in increase seen in every time point afterwards; particularly at 10 days of culture. Alamar Blue and Pico Green assays were used to calculate the metabolism per cell at each day. *$p<0.05$, **$p<.01$ ($n=4$, ANOVA).

Table 1
Compliance of the Human Umbilical Artery

Two sets of scaffolds were lathed at 250um, 500um, 750um, and 1000um thicknesses and tested for compliance. Significant difference of $p<0.05$ was observed between 250μm thickness samples and 750μm and $p<0.01$ for 1000μm thickness samples.

Scaffold Thickness (*t*)	Average Initial Outer Diameter (D_I)	Average Final Outer Diameter (D_F)	Diameter Change ($\Delta D/D$)	Compliance (average)
(μm)	(mm)	(mm)	(%)	(%/mm Hg)
250	4.77 ± 0.32	5.32 ± 0.56	11.47 ± 4.11	0.29 ± 0.09
500	5.74 ± 0.46	6.18 ± 0.44	7.83 ± 4.80	0.20 ± 0.14
750	7.57 ± 1.08	7.99 ± 0.88	5.75 ± 3.42	0.16 ± 0.11
1000	6.94 ± 0.69	7.11 ± 0.75	3.08 ± 1.84	0.07 ± 0.04

Table 2

Burst Pressure, % Diameter Change, and Compliance of Materials used for Small Diameter Vascular Grafts

Material	Burst Pressure (mm Hg)	Diameter Change (Δ*d*/*d*) (%)	Compliance (%/mm Hg)	Reference
Acellular Collagen	931 ± 284			Huynh, 1999 (37)
Aorta of Fetal Pigs	2493.13			Liu, 2008 (41)
Aorta of Fetal Pigs, Decellularized	2410.02			Liu, 2008 (41)
Artery, Femoral			0.06	Hastings, 1992 (31)
Carotid Artery, Porcine	3322.77 ± 412.53		0.187± 0.041	Dahl, 2007 (30)
Carotid Artery, Porcine	1987			McFetridge, 2004 (8)
Carotid Artery, Porcine, Crosslinked	2260			McFetridge, 2004 (8)
Carotid, Femoral, Iliac		15		Dobrin, 1978 (35)
DACRON		0.76		Sawyer, 1987 (34)
Dacron			0.02	Hastings, 1992 (31)
Dacron			0.019 ± 0.003	Zilla, 1998 (23)
Host Artery			0.059 ± 0.005	Zilla, 1998 (23)
Human Saphenous Vein	984			Kambric, 1984 (40)
Human Saphenous Vein	1680 ± 307			Veith, 1986 (26)
Human Saphenous Vein		1.96		Sawyer, 1987 (34)
Human Umbilical Artery	969.66 ± 154.42		0.0584 ± 0.0310	Gui, 2009 (18)
Human Umbilical Artery, Decellularized	840.37±114.67		0.0426 ± 0.0296	Gui, 2009 (18)
Human Umbilical Vein, Autodissected	1082 ± 113.4	4.6 ± 1.2		Daniel, 2005 (17)
Human Umbilical Vein, Autodissected, Decellularized	972.8 ± 133.8	5.7 ± 1.3		Daniel, 2005 (17)
Human Umbilical Vein, Manually Dissected		1.48		Sawyer, 1987 (34)
Human Umbilical Vein, Manually Dissected	699.2 ± 399.1	5.7 ± 2.1		Daniel, 2005 (17)
PGA Arteries	802.57 ± 105.01		.035 ± 0.002	Dahl, 2007 (30)
PGA scaffolds cultured in bioreactors for 5 weeks	570 ± 100			Niklason, 1999 (38)
PGA scaffolds cultured in bioreactors for 8 weeks	2150 ± 709			Niklason, 1999 (38)
PTFE		0.2		Stewart, 1987 (36)
PTFE		0.64		Stewart, 1987 (36)
PTFE			0.016 ± 0.002	Zilla, 1998 (23)
Small Intestinal Submucosa (SIS), Porcine, 5–8mm diam.	2069 – 4654	4.6, d=5mm 8.7, d=8mm		Roeder, 1999 (33)
TEBV made from SMCs and fibroblast sheets seeded with endothelial cells	2594 ± 501			L'Heureux, 1998 (39)
Umbilical Vein			0.037 ± 0.005	Zilla, 1998 (23)
Vein, Saphenous			0.04	Hastings, 1992 (31)